

## Retraction

# Retracted: Preparation of Ti Material Supported SBA-15 Functionalized with Sulfonic Acid Environmental Friendly Catalyst: Application for Esterification Process

### Journal of Nanomaterials

Received 11 July 2023; Accepted 11 July 2023; Published 12 July 2023

Copyright © 2023 Journal of Nanomaterials. This is an open access article distributed under the Creative Commons Attribution License, which permits unrestricted use, distribution, and reproduction in any medium, provided the original work is properly cited.

This article has been retracted by Hindawi following an investigation undertaken by the publisher [1]. This investigation has uncovered evidence of one or more of the following indicators of systematic manipulation of the publication process:

- (1) Discrepancies in scope
- (2) Discrepancies in the description of the research reported
- (3) Discrepancies between the availability of data and the research described
- (4) Inappropriate citations
- (5) Incoherent, meaningless and/or irrelevant content included in the article
- (6) Peer-review manipulation

The presence of these indicators undermines our confidence in the integrity of the article's content and we cannot, therefore, vouch for its reliability. Please note that this notice is intended solely to alert readers that the content of this article is unreliable. We have not investigated whether authors were aware of or involved in the systematic manipulation of the publication process.

Wiley and Hindawi regrets that the usual quality checks did not identify these issues before publication and have since put additional measures in place to safeguard research integrity.

We wish to credit our own Research Integrity and Research Publishing teams and anonymous and named external researchers and research integrity experts for contributing to this investigation.

The corresponding author, as the representative of all authors, has been given the opportunity to register their agreement or disagreement to this retraction. We have kept a record of any response received.

### References

- [1] R. Kalakuntala, M. Mekala, S. Chirra, V. Narayanan, V. R. Kakara, and S. Suranani, "Preparation of Ti Material Supported SBA-15 Functionalized with Sulfonic Acid Environmental Friendly Catalyst: Application for Esterification Process," *Journal of Nanomaterials*, vol. 2022, Article ID 6712464, 8 pages, 2022.

## Research Article

# Preparation of Ti Material Supported SBA-15 Functionalized with Sulfonic Acid Environmental Friendly Catalyst: Application for Esterification Process

Raju Kalakuntala <sup>1</sup>, Mallaiah Mekala <sup>2</sup>, Suman Chirra <sup>3</sup>, Venkatathri Narayanan <sup>3</sup>,  
Vighneswara Rao Kakara <sup>4</sup>, and Srinath Suranani <sup>1</sup>

<sup>1</sup>Department of Chemical Engineering, National Institute of Technology, Warangal 506004, India

<sup>2</sup>Department of Chemical Engineering, B V Raju Institute of Technology, Narsapur, 502313, India

<sup>3</sup>Department of Chemistry, National Institute of Technology, Warangal 506004, India

<sup>4</sup>Department of Chemical Engineering, Wollega University, Shambu Campus, Ethiopia

Correspondence should be addressed to Vighneswara Rao Kakara; vignesh.che@gmail.com

Received 23 December 2021; Revised 10 January 2022; Accepted 26 January 2022; Published 9 February 2022

Academic Editor: Karthikeyan Sathasivam

Copyright © 2022 Raju Kalakuntala et al. This is an open access article distributed under the Creative Commons Attribution License, which permits unrestricted use, distribution, and reproduction in any medium, provided the original work is properly cited.

Kinetics of catalytic esterification between propionic acid and n-butanol has been studied in a batch reactor by using a Ti-supported SBA-15 catalyst with sulfonic acid. The synthesized catalyst is used to test the efficacy of catalyst for esterification reaction. The SBA-15 acidity is tied to incorporation of Ti and  $-SO_3H$  groups through and the use of Si/Ti with Si/S molar ratios. The results are mesoporous materials with a typical hexagonal structure of the Ti SBA-15 and wide areas and high pore diameters that are operated with sulfonic groups. The addition of SBA to Ti leads mainly to catalytic materials with Bronsted and Lewis acid sites. Ti SBA-15 is the most effective catalyst for sulfonic acid, with the highest consents of Lewis acid sites and deactivation resistance and low hydrophilicity. The effect of temperature, catalyst amount, and molar ratio on reaction kinetics has been studied. The conversion of propionic acid is found to be 91% at 115°C at a 2:1 ratio of n-butanol to propionic acid molars with 2% of sulfonic acid supported Ti SBA-15. The Eley-Rideal kinetic model is used to fit the experimental data. The activation energy and kinetic factor are found to be 29.63 kJ mol<sup>-1</sup> and  $k_0$  0.549 L<sup>2</sup> g<sup>-1</sup> mol<sup>-1</sup>, respectively.

## 1. Introduction

Catalysis was first introduced as part of the growth of industrial technology in the 1960s, with a focus on refinery and petrochemical operations. Catalysis has advanced at a rapid rate over the last two decades, and it is now recognized as a multi-disciplinary discipline requiring synergistic interactions among a diverse spectrum of professionals, including materials, electrical, and mechanical engineers, physicists, biologists, and physicians. Catalysis provides and develops new, efficient, and cost-effective strategies and tools, as a leading technology toward a sustainable future and a clean environment, thereby improving people's quality of life [1].

In a multitude of goods, carboxylic acid esters are essential, from fragrances to biofuels. The latter would be of specific importance because of increasing crude oil prices and environmental issues. There are several hybrid routes for the production of organic esters [2]. The widely used technique for ester synthesis is an esterification reaction between carboxylic acids and alcohol. The reaction could be performed conventionally in batch reactors in a liquid state using powerful liquid nutrient acids like H<sub>2</sub>SO<sub>4</sub>, HI, and HCl as the catalyst [3, 4]. However, the handling strategy needs extra measures of catalyst removal and segregation with the substrate being disposed of salts, which usually adds to the processing cost. Alternatively, it is easy to separate strong catalysts from response products that can be used for various reaction cycles in most instances [4]. Furthermore, strong catalysts are used more readily in



ongoing processing activities, enhancing the ester manufacturing economy. For these reasons, the development of strong acid catalysts for esterification applications is of considerable concern [5]. The mathematical model and response mechanism for alkene esterification using homogeneous catalysts were well documented during a protonated methyl ester which was assaulted by a molecule of nucleophile alcohol, resulting in ester and water. With strong acid precursors containing mainly Bronsted acid clusters, esterification reaction could be expected with an analogous process to the homogeneous regime that mediates conversion [6, 7]. The results were uncertain in the literature on a basic strong acid-catalyzed esterification reaction. Two processes were suggested mainly for the esterification of heterogeneous catalysts. One is a single site mechanism, and the other one is a double site mechanism. Acetic acid esterification reaction with methanol by using SAC-13 was carried out with Bronsted acid sites as a single-site system. It is a gas stage with a range of temperatures of 90-140°C or within a condensed stage with temperature of 660°C, based on mainly the outcomes of studies with pyridine poisoning. An Eley-Rideal kinetic equation was developed to predict the experimental results with an accuracy of 8% for 1-octanol and hexanoic acid esterification utilizing zeolite and SAC-13 as catalysts [8].

The objective of the present research is the preparation and characterizations of an environmental catalyst for the esterification of propionic acid after the integration of Ti and sulfonic groups in SBA-15. The kinetics studies at different parameters have been carried out to find the conversion of propionic acid under various parameters. The Eley-Rideal model fitted with experimental data.

## 2. Experimental

**2.1. Catalyst Preparation.** Pluronic P123 is a discreet, linear substitute, triblock copolymer made up of polyethylene oxide (PEO) and polypropylene oxide (PPO). In an experiment 5 g of triblock copolymer (i.e., P123), structured mesoporous components such as SBA-15 are used as a backbone to be dispersed into distilled water of 116.25 g, and 29.13 g hydrochloric acid is inputted into the solution. Final 11 g of tetra-ethyl-ortho-silicate as a drug additive of silica was applied to tetraisopropoxide titanium (Si/Ti = 100) during steady 24-hour temperature mixing. The resulting slurry was accompanied by N-butanol and washed with distilled water. The material dried at 110°C for 12 hours and then calcined at 500°C for 8 hours [9].

**2.2. Characterization.** The pattern in the Ultima IV diffractometer is the powder X-ray diffraction (XRD). The following statistical figures are obtained within the range of 0.1-5° with a phase of 0.008° and a scanning speed of 0.5° per minute, using the nonfiltered Cu K $\alpha$  radiation source, in the form of a  $T = 0.54178 \text{ \AA}$  with 30 mA and 40 kV. TESCAN and VEGA 3 LMU, Australia, used for surface morphology study a scanning electron microscope (SEM). The photos of the samples were analysed with a 200 kv acceleration voltage using a tool JEOL Australia. Sample pores and surface area are specified in liquid nitrogen (77 K) and the

Chinese surface inspection system, Quanta Chrome Nova-1000, and also the de Boert map, BET, and pore size. Samples were obtained at 1:10 KBr room temperature with 10 scans from FTIR, PerkinElmer, Spectrum 100, USA. A Fourier transform spectra registered the samples [10]. On Evolution 300 Thermo Science, the sample spectrum was recorded with UV-visible spectrometer, USA, and BaSO<sub>4</sub> as reference, diffuse UV-visible spectrum (UV-Vis-DRS).

**2.3. Reaction Kinetics Study.** The reactor was filled with one mole of propionic acid and one mole of n-butanol. The heat input is supplied by rotating the heating knob to a desired temperature. The stirrer is adjusted to 480 rpm to mix the catalyst with reactants. When there is no temperature, the recalculated amount of catalyst is transferred into the reaction mixture. This time onwards the actual reaction time counted. The samples have been withdrawn in the regular intervals and analysed for propionic acid conversion by titration with standard NaOH solution. The reaction is continued till there is no change in the concentration of propionic acid concentration with time. This indicates the reaction reached chemical equilibrium.

## 3. Results and Discussions

The synthesized sulfonic acid-functionalized Ti SBA-15 catalyst is analysed for its characterization and used for kinetic investigations for reaction temperature of 85°C to 115°C, catalyst loading of 1 wt% to 3 wt%, and mole ratio of acid to alcohol 1:1 to 1:4.

**3.1. Transmission Electron Micrograph Analysis (TEM).** Figure 1 shows Ti-supported SBA-15 functionalized with sulfonic acid, revealing a hexagonally well-organized mesoporous catalyst with severe parallel channels, close to porous configuration. Ti-supported SBA-15 functionalized with sulfonic acid; TEM images functionalized with sulfonic acid [11]. In the long-range mesoporous ordering determined as opposed to the Ti-supported SBA-15 functionalized with sulfonic acid, there were uniform morphologies of the macrostructure of silica materials sulfonated.

**3.2. Diffuse Reflectance Ultraviolet-Visible Spectroscopic Analysis.** The Ti-supported SBA-15 functionalized with sulfonic acid spectrum of UV-Vis-DRS is shown in Figure 2. Two large peaks of ~210-230 nm and 330-350 nm were observed confined to the presence and integration of the tetrahedral environment and the homogeneous distribution of Ti ions in the Ti-supported SBA-15 functionalized with sulfonic acid matrix [12].

**3.3. Fourier Transform Infrared Spectroscopic Analysis (FTIR).** Figure 3 displays the Ti-supported SBA-15 functionalized with sulfonic acid composite FTIR spectrum of sulfonic acid. The 1088 cm<sup>-1</sup> peak suggests the Si-O-Si bond in a Ti SBA-15 fused sulfonated binding. The vibrations of Si-O-Si symmetrically stretching were 802 cm<sup>-1</sup> and 466 cm<sup>-1</sup>, respectively. Due to Ti-O-infrastructure Si's vibration, peaks 910 and 960 cm<sup>-1</sup> resulted, which means that Ti is strongly indicated in the SBA-15 matrix [13]. The exact

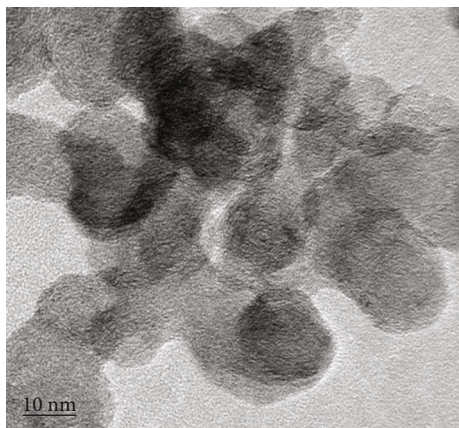


FIGURE 1: TEM images of Ti-supported SBA-15 functionalized with sulfonic acid.

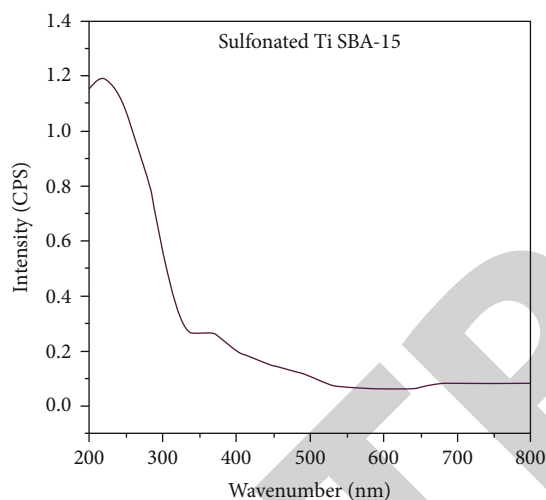


FIGURE 2: Ti-supported SBA-15 functionalized with sulfonic acid UV-Vis-DRS study.

location of the pictures was found to contribute both to the chemical composition and the calibration and resolution of the instrument used in the studies. In the Ti-supported SBA-15 functionalized with sulfonic acid catalyst, the maximum strength of the band is  $960\text{ cm}^{-1}$ . Due to hydrogen interaction, breaks between the silanol groups and the water molecules adsorbed were seen at  $1630$  and  $3400\text{ cm}^{-1}$  (SI-OH). The peaks of  $1052$  and  $1140\text{ cm}^{-1}$  confirm that the functional groups  $\text{-SO}_4\text{H}$  have symmetrical and asymmetrical vibrations.

**3.4. Powder X-Ray Diffraction (XRD).** Synthesized sulfonic acid pattern of powder X-ray diffraction (XRD) composites functionalized by Ti-supported SBA-15 shown in Figure 4. In the X-ray diffraction study, two weak peaks and a strong, extreme peak were noted [14]. The weak peaks found by  $2\theta$  were  $1.4$  and  $1.7$ , and the sharp peak by  $2\theta$  was  $0.8$ , which specify the periodicity of the high structures as a result of higher condensation between the silanol and titanium groups.

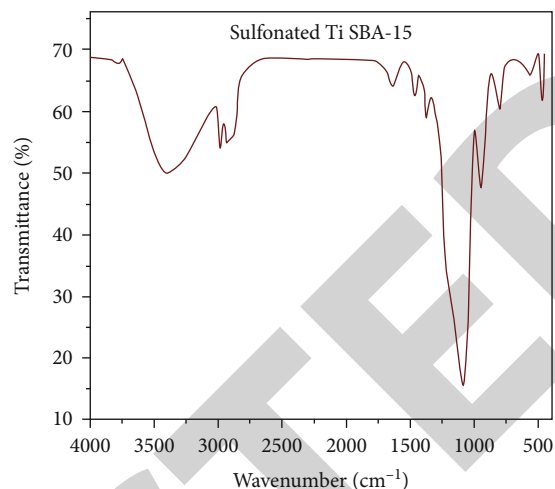


FIGURE 3: FT-IR analysis of Ti-supported SBA-15 functionalized with sulfonic acid.

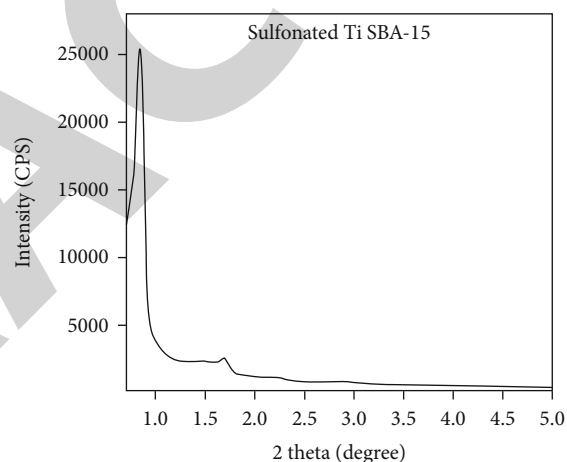


FIGURE 4: Small-angle XRD pattern of Ti-supported SBA-15 functionalized with sulfonic acid.

**3.5. Thermogravimetry/Differential Thermal Analysis.** Figures 5 and 6 display the Ti-supported SBA-15 functionalized with sulfonic acid materials from the TG-DTA analysis of sulfonic acid. It explains preliminary weight loss from  $0^\circ\text{C}$  to  $300^\circ\text{C}$  (4.31%) by loss in mesoporous composite of water adsorbed and ethanol molecules [15]. Therefore, the decomposition of the pattern that is trapped within the Ti-supported SBA-15 functionalized with sulfonic acid and its remainder shown to be steep weight loss between  $350^\circ\text{C}$  and  $600^\circ\text{C}$  is 29.86% to 58.75%.

The DTA plot proposed that the patterns of the mesoporous material should be heated. A weight loss of initial  $0^\circ\text{C}$  to  $300^\circ\text{C}$  of  $0^\circ\text{C}$  is observed in the data track of the sulfonic acid functionalized composite Ti-SBA-15 (4.06%). A further weight loss in sulfonic acid pores of Ti-SBA-15 (42.89%) was found to be 52.3% due to the oxidative decomposition of obstructed patterns, and residual mass was 52.3%. A large exothermic peak at  $308.7^\circ\text{C}$  has been reported. The Ti-supported SBA-15 functionalized with sulfonic acid composite has no weight loss observed in  $500\text{-}700^\circ\text{C}$ . These Ti-

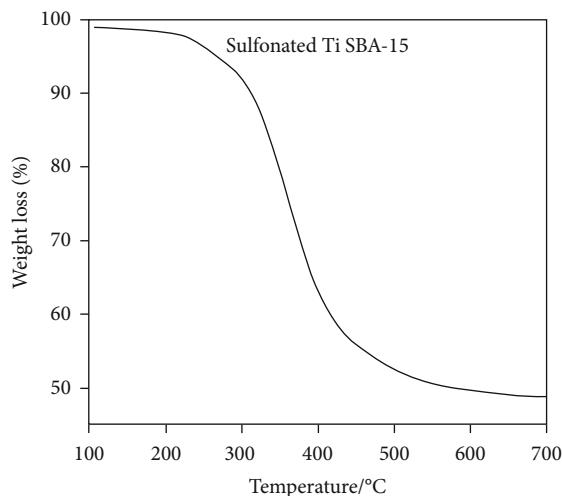


FIGURE 5: TGA analysis of Ti-supported SBA-15 functionalized with sulfonic acid.

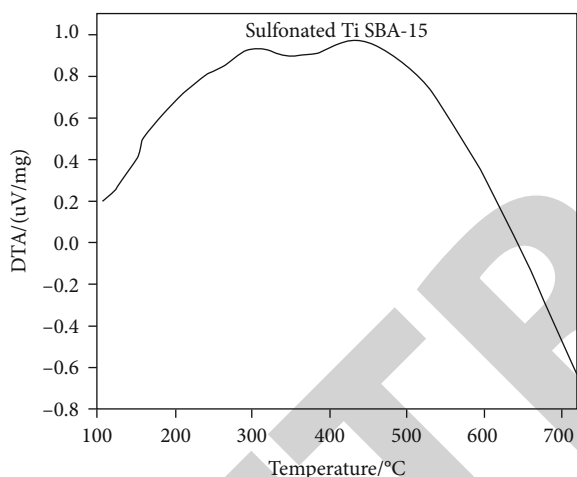


FIGURE 6: DTA analysis of Ti-supported SBA-15 functionalized with sulfonic acid.

SBA-15 composites with sulfonic acid function are also thermally stable up to 700°C.

**3.6.  $N_2$  Adsorption-Desorption Studies.** Information on the surface area, the pores of composites Ti-supported SBA-15 functionalized with sulfonic acid have been provided through adsorption isothermal studies and is shown in Figure 7. Subsequently, it was noted that the silicon composites were shown to indicate their mesoporosity as the type IV nitrogen isotherms with the deposal H1 hysteresis loop [16]. The distribution of mesoporous sizes extends when the Ti is incorporated in the SBA-15 framework. These results have been validated using the distribution curve for pore size. The results show that when the Ti was integrated into the SBA-15 functionalized with sulfonic acid framework, the consistency of the mesoporous size distribution has declined. It was also noted that the pore volume, surface area, pore diameter, and also peak intensities were decreased sharply with increased incorporation of Ti into the SBA-15 functionalized with sulfonic

acid samples [17]. This could be due to the blocking by titanium-based mesoporous canals. In order to define the texture properties of the mesoporous catalysts, the BJH pore size distribution approach and the BET surface analysis are employed in Table 1.

## 4. Catalytic Performance (Sulfonic Acid Functionalized Ti SBA-15)

**4.1. Effect of Reactant Molar Ratio.** The mole ratio of propionic acid with n-butanol varied from 1:1 to 1:4 at a temperature of 115°C and a speed of 240 rpm for conversion of propionic acid with Ti-supported SBA-15 functionalized with sulfonic acid [18]. The conversion of propionic acid as function of molar ratio is shown in Figure 8. The propionic acid conversion increases as the molar ratio increases due to excess n-butanol. From the figure, it could be observed as 79.90%.

**4.2. Effect of Temperature.** The effect temperature on the conversion of propionic acid at 2% by wt catalyst loading and at 1:1 mole ratio is shown in Figure 9. The conversion of propionic acid is increased as temperature increases. Higher the temperatures, the time required to reach equilibrium is lesser [19]. It shows that the reaction is kinetically controlled.

**4.3. Effect of Catalyst Amount.** The effect of catalyst amount on the propionic acid conversion kinetics is shown in Figure 10 at a temperature of and mole ratio of 1:1. The experiments employ separate catalyst concentrations of 1, 2, and 3 wt%. The conversion of propionic acid increases as the catalyst loading increases [20]. When the catalyst quantity increased in the reaction mixture, the reaction rate increases due to availability of  $H^+$  ions which in turn provide more catalyst surface area. The experiments were conducted for 4 runs with the same catalyst. The propionic acid conversion is the same under 1% error.

**4.4. The Ti-Supported SBA-15 Functionalized with Sulfonic Acid for the Kinetic Analysis.** The initial reaction rate of propionic acid with n-butanol has been carried out under different catalyst loadings ( $r_{A0} = \Delta C_{A0}/\Delta t$ ) for this catalyst [21]. The general kinetic expression for the catalyzed heterogeneous esterification reaction can be written as

$$-r_A = \frac{k_f w_{\text{cat}} (C_A C_B - (C_R C_w / K_{eq}))}{(1 + K_A C_A + K_B C_B + K_E C_E + K_w C_w)^n}, \quad (2)$$

where  $r_A$  is the reaction rate and ( $w_{\text{cat}}$ ) is the catalyst weight on dry basis. A, B, E, and W represent propionic acid, n-butanol, butyl propionate, and water. K is the adsorption constant,  $K_e$  is the equilibrium constant, and  $k_f$  is the forward reaction rate constant. In equation (2), when  $n = 0$ , it is a PH model; when  $n = 1$ , it is ER model; and when  $n = 2$ , it is a LHHW model.

As can be seen in Figure 11, the starting reaction rate instead of the plated one is a linear feature, which means the adsorption of propionic acid on the Ti-supported

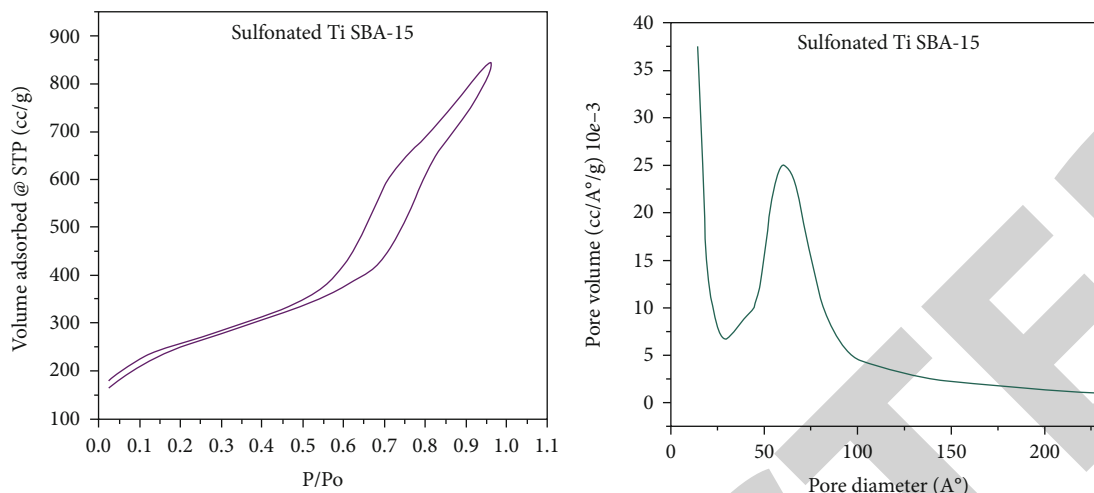


FIGURE 7: Ti-supported SBA-15 functionalized with sulfonic acid with  $N_2$  adsorption/desorption isotherms, pore diameter, and pore volume distribution.

TABLE 1: BET-isothermic adsorption and porosity data.

Mesoporous material	Pore volume (cc/g)	Average pore diameter ( $\text{\AA}$ )	Surface area ( $\text{m}^2/\text{g}$ )
Ti-supported SBA-15 functionalized with sulfonic acid	1.02	31.78	457

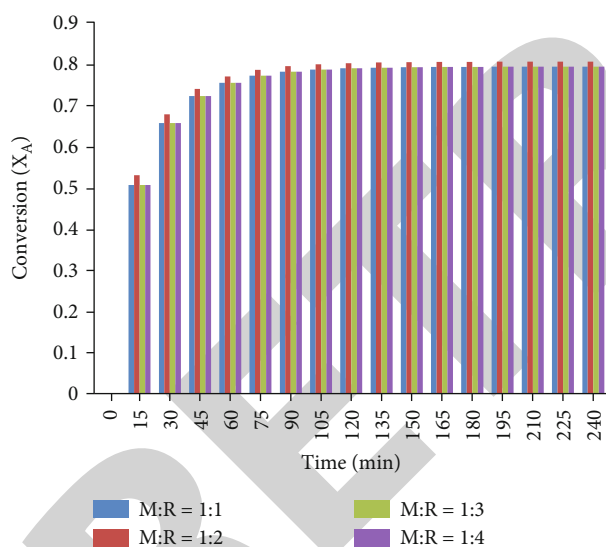


FIGURE 8: Conversion versus time for different molar ratios. Other conditions are catalyst loading: 2%, temperature:  $115^\circ\text{C}$ , and speed: 240 rpm.

SBA-15 functionalized with sulfonic acid catalyst surface is not possible, and at the same time, the initial rate of reaction increases in line with n-butanol concentrations. Therefore, we can infer that at low concentrations of n-butanol, it adsorbed n-butanol extremely low and almost continuously increases the concentration. This study concludes that the reaction mechanism is defined in the Eley-Rideal model, i.e., reaction between adsorbed butanol molecules and propionic acid molecules in the bulk solution. In the single site, only one reactant is adsorbed on

the catalyst and the remaining reactant is in the bulk reaction. In the double site, two reactants are at the catalyst surface and reaction proceed at this place and formed products desorbed from the catalyst surface. The literature found the solvent (dioxane) and ester adsorption to be insignificant. The rate determination step is to specifically take the stoichiometric and corresponding reaction rate as the Eley-Rideal (ER) model of a surface-reaction equation. After excluding terms of adsorption of acid and ester, ER form can be written as

$$-r_A = \frac{k_f w_{\text{cat}} (C_A C_B - (C_R C_w / K_{eq}))}{(1 + K_B C_B + K_w C_w)} \quad (3)$$

The Arrhenius law expresses the dependence of temperature on reaction rate as given in the following.

Equation (3) behavior is used for speed expression rather than concentration, because the predictions of models adapted to the measured film data result in improved prediction [22]. Relocation of equation (4) can be described as equation for the initial reaction rate without a product present, shown in

$$\frac{C_{A_0} C_{B_0}}{-r_{A_0}} = \frac{1}{(k_f w_{\text{cat}})} + \frac{K_B}{k_f w_{\text{cat}}} C_{B_0} \quad (4)$$

Figure 12 shows the plot of  $C_{A_0} C_{B_0} / -r_{A_0}$  versus  $C_{B_0}$  results in a direct slope line  $K_B / k_f w_{\text{cat}}$  and intercept  $1 / k_f w_{\text{cat}}$  as shown in the figure.

Slopes and intercepts in these figures indicate the constants in rates and adsorption constants  $k_f$ ,  $K_B$ ,  $K_w$ , and their estimated values at three temperatures as shown in Table 2.

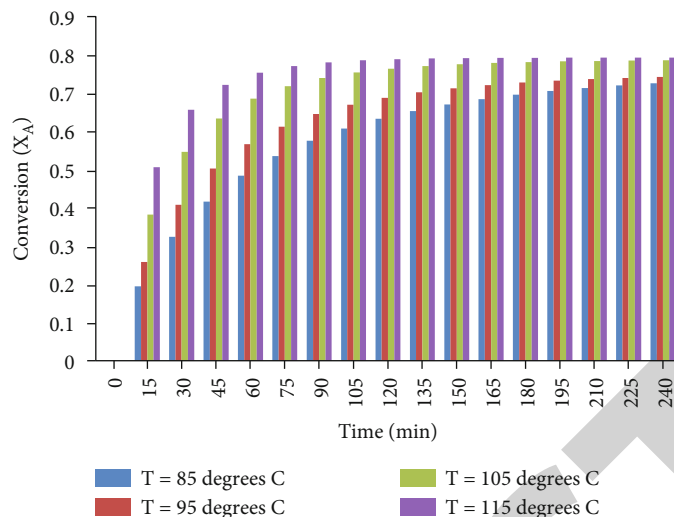


FIGURE 9: Conversion versus time for different temperatures. Other conditions are catalyst loading: 2%, mole ratio: 1 : 1, and speed: 240 rpm.

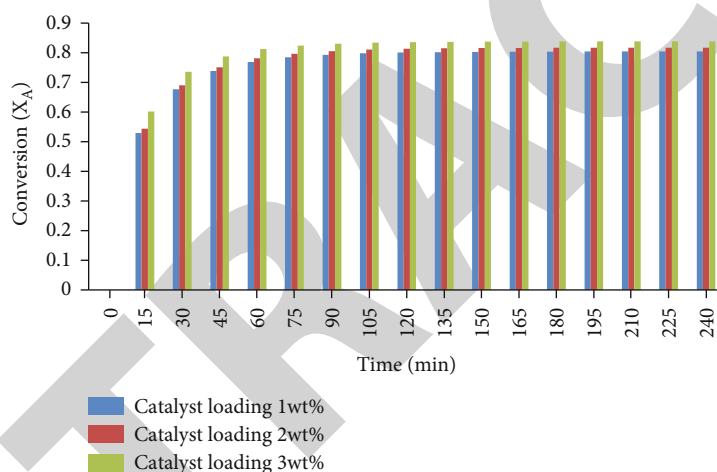


FIGURE 10: Conversion vs. time (min) for different catalyst loadings. Other conditions are mole ratio: 1 : 1, temperature: 115°C, and speed: 240 rpm.

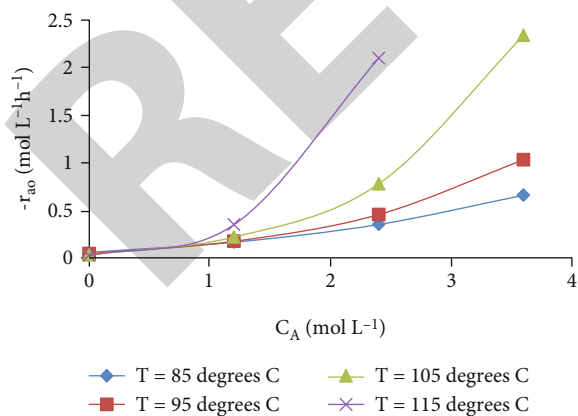


FIGURE 11: The effect on the initial reaction rate of ( $-r_{A0}$ ) at different temperatures on the charging of catalyst.

4.5. *Activation Energy and Rate Constants.* The Arrhenius law expresses the dependence of temperature on reaction rate as given in the following:

$$k_i = k_i^0 \exp(-E_i/RT), \quad (5)$$

where  $k_f$  is the activation energy for forward reaction and  $k_{i0}$  is the frequency factor [23]. Equation (5), a plot of  $\ln K_F$ ,  $\ln K_B$ , and  $\ln K_W$  versus  $1/T$  plot, lists a slope straight of  $(E/R)$  and, as shown in Figure 13,  $\ln k_{i0}$  intercept opposed to  $1/T$ . In the presence of sulfonic acid functionalized Ti SBA-15, the activation energy was found to be 39.5 kJ mol<sup>-1</sup>. The adsorption constants as function of temperature have arrived from Figure 13 as given in equations (7)–(9).

$$K_F (\text{L}^2 \text{g}^{-1} \text{mol}^{-1} \text{h}^{-1}) = \exp^{(232-1109/T)}, \quad (6)$$

$$K_B (\text{L mol}^{-1}) = \exp^{(3125/T-17.83)}, \quad (7)$$

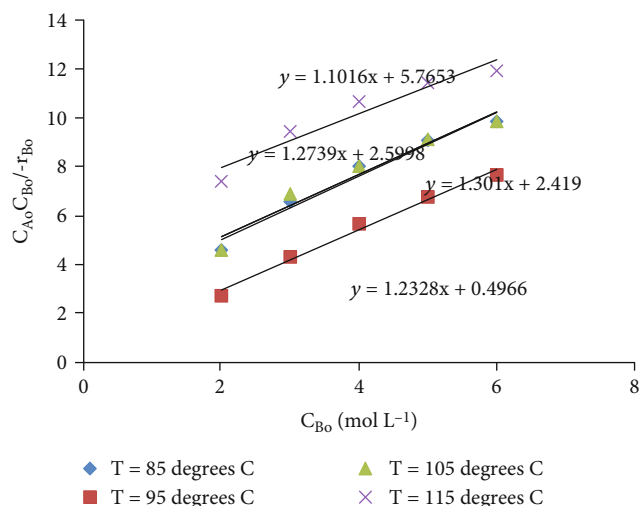


FIGURE 12:  $C_{A_0} C_{B_0} / -r_{A_0}$  versus  $C_{B_0}$  at different temperatures.

TABLE 2: Kinetics and adsorption constants.

Temperature (°C)	$k_f / L^2 mol^{-1} h^{-1}$	$K_B / L mol^{-1}$	$K_W / L mol^{-1}$
85	$0.78 \times 10^{-4}$	0.18	0.19
95	$0.81 \times 10^{-4}$	0.20	0.49
105	$0.78 \times 10^{-4}$	0.19	0.51
115	$0.90 \times 10^{-4}$	0.09	0.56

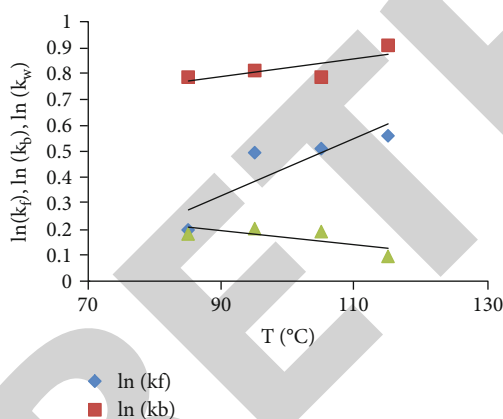


FIGURE 13: Arrhenius plot for  $\ln K_b$ ,  $\ln k_f$ , and  $\ln K_w$  vs.  $T$ .

$$K_w (L mol^{-1}) = \exp^{(4856/T - 54.9)}. \quad (8)$$

4.6. *Model Prediction.* Model predictions with ER model have been compared with experimental results as shown in Figure 14, for esterification of propionic acid with butanol over an entire range of expected parameters [24].

The following equation (9) is used to determine the experimental reaction rate for different time steps for various acid conversions.

$$-r_{A,\text{experimental}} = \frac{\Delta C_A}{\Delta t} = C_{A_0} \frac{\Delta X}{\Delta t}. \quad (9)$$

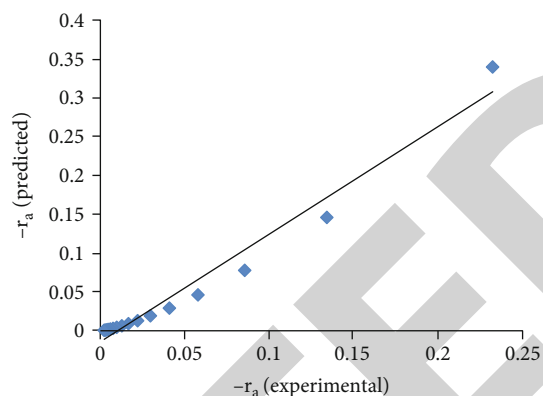


FIGURE 14: Parity plot for rate of reaction from experimental data and model prediction.

Figure 14 shows the parity plot between the experimental value and the calculated values. It can be observed that the findings fall within  $\pm 5$  percent error.

## 5. Conclusions

SBA-15, Ti, and  $-SO_3H$  were successfully incorporated with a sol-gel process. It is found that final Ti-and-S contents were less than anticipated in samples. Moreover, the presence of sulphur decreases titanium's inclusion in the SBA-15. Propionic acid reaction kinetics with n-butanol has been investigated with this catalyst. Experimental results indicate that the reaction is kinetic controlled instead of mass transfer controlled. Eley-Rideal (ER) was developed based on an adsorption analysis to interpret kinetic data. The kinetic model was well prepared with experimental results. The EA 29.63 kJ/mol activation energy and kinetic factor  $k_0$  0.549 L<sup>2</sup>/g-mol-h were found.

## Data Availability

No data were used to support this study.

## Conflicts of Interest

The authors declare that they have no conflicts of interest regarding the publication of this paper.

## References

- [1] I. V. Yentekakis and F. Dong, "Grand challenges for catalytic remediation in environmental and energy applications toward a cleaner and sustainable future," *Frontiers in Environmental Chemistry*, vol. 1, pp. 1–14, 2020.
- [2] A. Chakrabarti and M. M. Sharma, "Cationic ion exchange resins as catalyst," *L' Azione sanitaria*, vol. 20, no. 1-2, pp. 1–45, 1993.
- [3] V. H. Agreda, L. R. Partin, and W. H. Heiss, "High purity methyl acetate via reactive distillation," *Chemical Engineering Progress*, vol. 86, no. 2, pp. 40–46, 1990.
- [4] R. Ronnback, T. Sami, A. Vuori et al., "Development of a kinetic model for the esterification of acetic acid with

- methanol in the presence of a homogeneous acid catalyst," *Chemical Engineering Science*, vol. 52, no. 19, pp. 3369–3381, 1997.
- [5] M. R. Altiokka and A. Citak, "Kinetics study of esterification of acetic acid with isobutanol in the presence of amberlite catalyst," *Applied Catalysis A: General*, vol. 239, pp. 141–148, 2003.
- [6] B. Erdem and M. Cebe, "Kinetics of esterification of propionic acid with n-amyl alcohol in the presence of cation exchange resins," *Korean Journal of Chemical Engineering*, vol. 23, pp. 896–901, 2006.
- [7] H. T. R. Teo and B. Saha, "Heterogeneous catalysed esterification of acetic acid with isoamyl alcohol: kinetic studies," *Journal of Catalysis*, vol. 228, no. 1, pp. 174–182, 2004.
- [8] Y. Liu, E. Lotero, and J. G. Goodwin Jr., "A comparison of the esterification of acetic acid with methanol using heterogeneous versus homogeneous acid catalysis," *Journal of Catalysis*, vol. 242, no. 2, pp. 278–286, 2006.
- [9] E. Casas, R. van Grieken, and J. M. Escola, "Polymerization of ethylene with (nBuCp)<sub>2</sub>ZrCl<sub>2</sub> supported over mesoporous SBA-15 functionalized with sulfonic acid groups," *Applied Catalysis A: General*, pp. 44–52, 2012.
- [10] R. H. Vekariya and H. D. Patel, "Sulfonic acid-functionalized silica (SiO<sub>2</sub>-Pr-SO<sub>3</sub>H) as a solid and a heterogeneous catalyst in green organic synthesis: recent advances," *Synthetic Communications*, vol. 45, no. 9, pp. 1031–1054, 2015.
- [11] D. Srinivas and P. Ratnasamy, "Spectroscopic and catalytic properties of SBA-15 molecular sieves functionalized with acidic and basic moieties," *Microporous and Mesoporous Materials*, vol. 105, no. 1-2, pp. 170–180, 2007.
- [12] D. A. Cabrera-Munguia, H. González, E. T. Rios, A. G. Alejandre, and J. L. Rico, "Acid properties of M-SBA-15 and M-SBA-15-SO<sub>3</sub>H (M = Al, Ti) materials and their role on esterification of oleic acid," *Journal of Materials Research*, vol. 33, no. 21, pp. 3634–3645, 2018.
- [13] B. François, A. Khadhraoui, M. T. Janicke, F. Kleitz, and S. Kaliaguine, "Optimizing silica synthesis for the preparation of mesoporous Ti-SBA-15, epoxidation catalysts," *Industrial & Engineering Chemistry Research*, vol. 49, pp. 6977–6985, 2010.
- [14] A. Okamoto, R. Nakamura, H. Osawa, and K. Hashimoto, "Site-specific synthesis of oxo-bridged mixed-valence binuclear complexes on mesoporous silica," *Langmuir*, vol. 24, pp. 7011–7017, 2008.
- [15] H. Rita, *Synthesis, characterization and catalysis of nanostructured vanadia model catalysts for partial oxidation of propane*, Technische Universität Berlin, 2009.
- [16] J. Melero, R. van Grieken, and G. Morales, "Advances in the synthesis and catalytic applications of organosulfonic-functionalized mesostructured materials," *Chemical Reviews*, vol. 106, no. 9, pp. 3790–3812, 2006.
- [17] X. Guo, Q. Cao, Y. Jiang, J. Guan, X. Wang, and X. Mu, "Selective dehydration of fructose to 5-hydroxymethylfurfural catalyzed by mesoporous SBA-15-SO<sub>3</sub>H in ionic liquid BmimCl," *Carbohydrate Research*, vol. 351, pp. 35–41, 2012.
- [18] M. Kulawska, M. Organek, and W. Organek, "Catalytic esterification of medium-chain fatty acids: kinetic investigations," *International Journal of Organic Chemistry*, vol. 7, no. 4, pp. 336–345, 2017.
- [19] G. D. Yadav and P. H. Mehta, "Heterogeneous catalysis in esterification reactions: preparation of phenethyl acetate and cyclo-hexyl acetate by using a variety of solid acidic catalysts," *Industrial & Engineering Chemistry Research*, vol. 33, pp. 2198–2208, 1994.
- [20] G. Jyoti, A. Keshav, J. Anandkumar, and S. Bhoi, "Homogeneous and heterogeneous catalyzed esterification of acrylic acid with ethanol: reaction kinetics and modeling," *International Journal of Chemical Kinetics*, vol. 50, pp. 370–380, 2018.
- [21] A. Citak, *Application of ion exchange resins in the synthesis of isobutyl acetate, ion exchange technology II*, Springer Nature, 2012.
- [22] M. J. Lee, J. Y. Chiu, and H. Lin, "Kinetics of catalytic esterification of propionic acid and -butanol over Amberlyst 35," *Industrial & Engineering Chemistry Research*, vol. 12, pp. 2882–2887, 2002.
- [23] M. Z. Ghodsi, N. Lashgari, and A. Badiei, "Sulfonic acid-functionalized mesoporous silica (SBA-Pr-SO<sub>3</sub>H) as solid acid catalyst in organic reactions," *Journal of Molecular Catalysis A: Chemical*, vol. 397, pp. 166–191, 2015.
- [24] Y. Liu, Z. Zhou, G. Yang, Y. Wu, and Z. Zhang, "Kinetics study of direct hydration of dihydromyrcene in a jet reactor," *Industrial & Engineering Chemistry Research*, Vol. 7, pp. 3170–3175, 2010.